CRYSTAL GROWTH & DESIGN
2006
VOL. 6, NO. 6
1415−1419

Computing Shapes of Nanocrystals from X-ray Diffraction Data

Daniel Sherwood and Bosco Emmanuel*

Modeling & Simulation Group, Central Electrochemical Research Institute, Karaikudi-630 006, India

Received January 30, 2006; Revised Manuscript Received February 28, 2006

ABSTRACT: An elegant mathematical technique has been developed and tested for computing the shapes of nanocrystals from X-ray diffraction (XRD) data. The method is specially suited to the shape analysis of crystallites in nanopowder specimens. Unlike visualization techniques such as transmission electron microscopy (TEM), it can find the full 3-D crystallite shape even in the presence of agglomeration. The technique has been validated using XRD and TEM data on the systems CeO_2, Ge, ZnO, $Zr_{56}C_{44}$, In_2O_3, $MnFe_2O_4$, and iron(II−III) hydroxysulfate. This will aid in the shape-selective synthesis and design of materials. Other merits of the method and some extensions are also discussed.

Introduction

Crystals and their shapes have been a fascination of man from the olden times when minerals were in fact recognized by their distinct crystal shapes. Today, the shape control of nano- and microcrystals is an important goal of modern materials[1] chemistry as different shapes of the particles[2] can introduce different electronic, optical, and magnetic properties with ramifications in a variety of physical, chemical, and biological processes, phenomena, and applications. In particular, the control of nanocrystal shape remains an interesting and important topic in nanoparticle research due to the coupling between shape and properties at the nanometer scale.[3] To-date, shape-controlled synthesis has been achieved for many metals and alloys, such as Pd,[4] Co, Ag, Au, Pt, and FePt.[5] Palladium nanoparticles of several morphologies have been synthesized in the presence of surfactants[6] and with the mediation of RNAs.[7] By tailoring the shape, one can enhance their catalytic performance in a range of applications.[8] Semiconductor[2] nanoparticles have been made in various shapes that are interesting for quantum[9] confinement studies and useful for potential sensor, transistor, and solar cell applications. Ceramics, including a host of oxide materials, and organic crystals are two other areas where the crystal shape is of critical importance. On the biology front, the biological availability[10,11] of drugs depends critically on the dissolution rate of particles, which in turn is determined by their shapes. Similarly, biomineralization[12−14] relies on the crystallization of specific morphologies of inorganic minerals.

The shapes of crystals depend on a host of environmental factors such as the solvent,[15] solution chemistry,[16] pH,[15,17−19] surface-active agents,[20] temperature,[15,17,19,21,22] and additives ranging from a single atomic ion[23] right through to a protein. These factors act by differentially modulating either the surface energies (cf. equilibrium crystal shapes and Wulff's construction) or the relative rates of growth of different faces. For example, the growth of copper nanocrystals as cubes,[24] the perovskite $BaZrO_3$[25] as rhombic dodecahedrons, and the three different shapes of tricalcium aluminate[26] were traced, respectively, to chloride ion adsorption on (100) faces, solvent-induced polarity variation, and the presence of the three growth modifiers, sulfate, oxalate, or EDTA, each one having a strong affinity to a different face of the crystal.

Platinum[27] nanocrystals with three different shapes, cubes, cubooctahedra, and octahedra, are reported where the addition of silver ion enhances the crystal growth along ⟨100⟩ and essentially determines the crystal shape. RNA-mediated metal−metal bond formation was interestingly shown to change the growth habit of palladium particles, which are usually cubic, to thin hexagonal crystallites.[7] Formation of chiral[28] morphologies through selective binding of amino acids to calcite surface is another interesting finding. The crystal morphology of calcite grown in the presence of one enantiomer of aspartic acid is the mirror image of that found when the crystals are grown in the presence of the other enantiomer.

A Mathematical Algorithm for Computing Crystal Shapes from X-ray Diffraction Data

A set of well-developed mathematical methods is available today that can cull a wide range of information from X-ray diffraction data. The Rietveld refinement is the single most prominent technique used to compute the internal crystal structure[50] (including the space group, the unit cell parameters, and the atomic/ionic positions within the unit cell).

Despite the tremendous success of X-ray crystallography as an experimental tool, an important characteristic of crystals that is yet to be brought within its purview is the external crystal shape (known also as morphology or habit). A material of a given internal symmetry may crystallize in several different crystal shapes depending on the experimental conditions of its growth/synthesis. A classic example is the growth of NaCl crystals in varying concentrations of urea that modify the crystal habit[29] (see Figure 4 in Supporting Information).

Several models have also been advanced for crystal shape prediction, two early models being the Wulff construction[30−32] and the Bravais−Friedel−Donnay−Harker (BFDH)[33,34] method. Later refinements of the BFDH led to the so-called periodic bond chain model[35] and the attachment energy model.[36] More recently, molecular dynamics simulations as well as Monte Carlo algorithms have been successfully used to predict the shapes of urea crystals,[37] monoclinic paracetamol crystals,[15] amino acids[38] (α-glycine and L-alanine), and the morphological importance of faces in the gibbsite crystal[39] (γ-$Al(OH)_3$). Unlike these models, which aim to predict crystal shapes, the present mathematical algorithm is designed to compute crystal shapes as actually realized in experiments. Hence this algorithm helps the experimental researcher to compute crystal shapes from his XRD data, and the theoretician to validate his model predictions.

Traditionally, equipment such as the transmission electron microscope (TEM) provides the crystal shape information as

* Corresponding author. Member, American Chemical Society.

10.1021/cg060052l CCC: $33.50 © 2006 American Chemical Society
Published on Web 04/27/2006

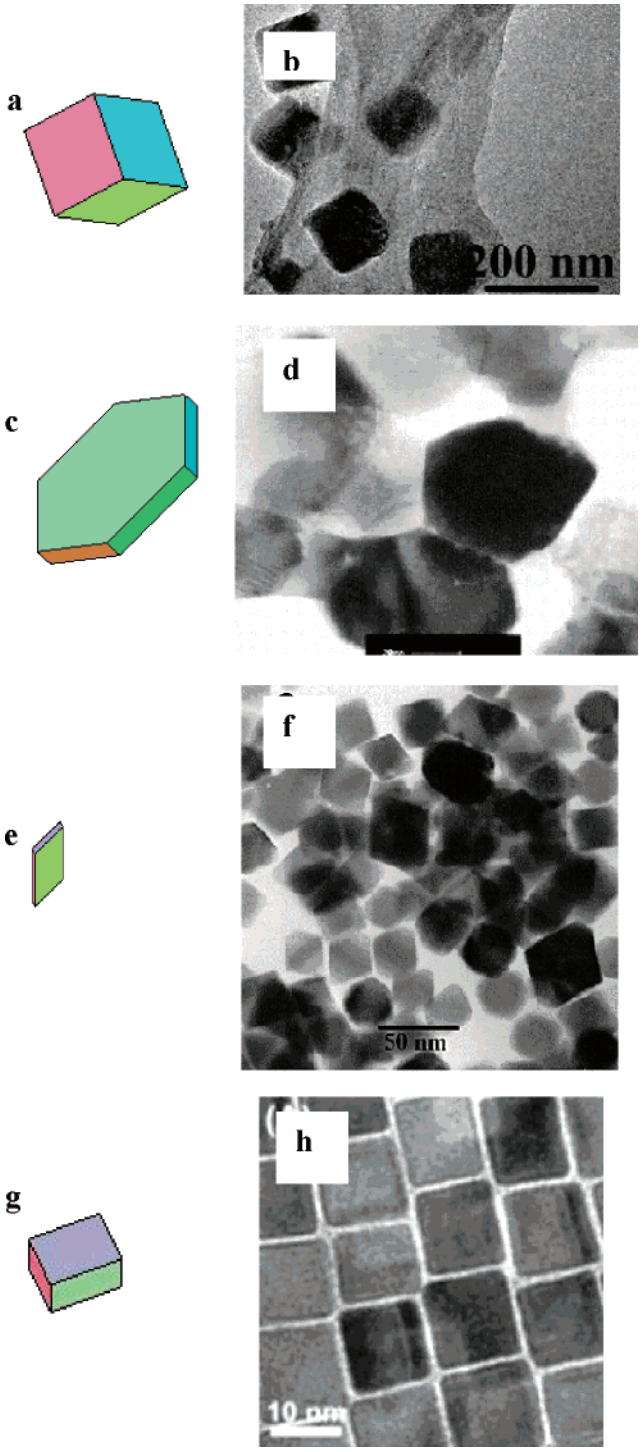

Figure 1. Some crystal shapes computed by the present mathematical algorithm and validated using the available TEM. Panel a shows the computed crystal shape of Ge nanocrystal. In panel b, the TEM picture shows nearly cubic nanocrystals, synthesized using $C_{12}E_7$ as a shape-controlling agent. The XRD is taken and TEM is reproduced from ref 41. Copyright 2005 American Chemical Society. Panel c shows the computed crystal shape of ZnO nanocrystal. In panel d, the shape agrees well with TEM though one or two crystals are distorted from the perfect hexagonal shape. The XRD is taken and TEM is reproduced with permission from ref 42. Copyright 2004 Elsevier. Panel e shows the computed crystal shape of In_2O_3 nanocrystal. Panel f displays the TEM picture showing crystals of square and rhombohedral shape. The XRD is taken and TEM is reproduced from ref 44. Copyright 2004 American Chemical Society. Panel g shows the computed shape of $MnFe_2O_4$. In panel h, the TEM shows the top view of cubic-like crystals lying flat. The XRD is taken and the TEM is reproduced from ref 2. Copyright 2004 American Chemical Society.

visual photographs. Though the semiquantitative visual information contained in these may be adequate for routine materials development work, quantitative methods are clearly desirable for gathering more information about the crystal shape. For instance, assigning an unique Miller index (*h*,*k*,*l*) to each of the crystal faces exposed in TEM is not straightforward. Besides, these equipments provide only projected 2D information and not the complete 3D information, because one cannot view the crystals from arbitrary angles, and only the crystal faces exposed to the instrument's camera will be accessible for inspection.

The crystal shape information that we propose to extract from XRD data consists of (1) the number and types of crystal faces exposed, (2) the geometrical area of each exposed crystal face, and (3) the complete 3-D shape of the crystal.

The basic inventive step in the development of the said mathematical algorithm consisted in the observation that, in an XRD, each diffraction peak arises from a set of well-defined crystal planes and the peak width is related, through the Scherrer formula, to the thickness of the crystal in a direction perpendicular to these set of planes and realizing that the crystal shape is actually given by the mathematical envelope formed by the pairs of parallel planes, each pair corresponding to a diffraction peak and the distance of separation of the two planes in the pair being related to the peak width. It is to be noted that each pair of parallel planes has a orientation in space given by the Miller index of the corresponding diffraction peak. Hence the inputs to the crystal shape algorithm are the Miller index (*h*,*k*,*l*), the 2θ-value and the peak width at half-maximum for each diffraction peak, and the unit cell parameters (a, b, c and α, β, γ).[51] Note that these parameters are obtainable from standard methods. Except the peak-width data, these need to be fixed only once for any given material; the peak-width data alone will vary from one crystal shape to another for the same material, depending on the conditions of synthesis.

The peak width at half-maximum, B_{hkl}, for a diffraction peak with the Miller index (*h*,*k*,*l*) is inversely related by the Scherrer formula

$$B_{hkl} = \frac{0.9\lambda}{t_{hkl} \cos \theta_{hkl}}$$

to the crystal thickness, t_{hkl}, in a direction normal to the *hkl* plane. Hence the diffraction peaks will be quite narrow for large crystals and broad for nanocrystals. Though the proposed algorithm is equally applicable for all crystal sizes, corrections for instrumental and other extraneous broadening are conveniently done for broader diffraction peaks. So this algorithm is better suited to finding the crystal shapes of nanomaterials. The mathematical steps of the algorithm are summarized below, and the details are provided in the Supporting Information.

The method starts with a duly indexed XRD pattern. The crystal system and the unit cell parameters are found using available standard methods. With use of the 2θ-value and the peak width at half-maximum (i.e., B value) for each of the XRD peaks, the crystal thicknesses, t_{hkl}, in different directions are computed using the Scherrer formula

$$t_{hkl} = \frac{K\lambda}{B_{hkl} \cos \theta_{hkl}}$$

where K is the Scherrer constant and λ is the wavelength of the X-ray. The set of crystal planes defined by the set of t_{hkl}'s is used to determine the mathematical envelope for the crystal shape. Computing this mathematical envelope involves the following steps: (i) a complete enumeration of the points of

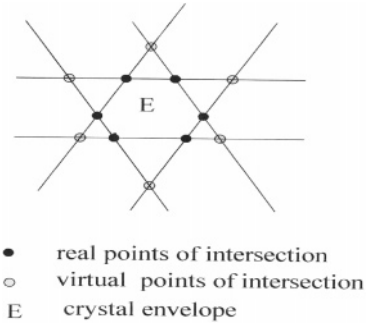

Figure 2. Real and virtual points of intersection and the corresponding crystal envelope. This illustration is given in 2-D for simplicity, though the actual mathematical algorithm works in 3-D.

intersections of the crystal planes defined by the set of t_{hkl}'s, (ii) identification and discarding of the virtual points of intersections that lie outside the envelope (see Figure 2), (iii) finding the set of real points of intersection that fall on each crystal face (note that this set will be a null set if the corresponding crystal face is not expressed in the crystal envelope), (iv) while we now possess a set of polygons oriented in space according to their Miller indices, computing the area of each polygon that gives the area of the corresponding crystal face, and (v) since this set of polygons span the crystal boundary, determining the 3D-shape of the crystal. The mathematical details of the method are given in the Supporting Information.

Crystal Shapes Computed from XRD

For applying the crystal shape algorithm, we start with a good quality XRD data of the material, a set of parameters are extracted from the XRD data and are fed into the crystal shape algorithm. As output, the algorithm generates the Miller indices of the crystal faces exposed, the area of each exposed face, and the complete three-dimensional view of the crystal that can be rotated to any arbitrary orientation. The detailed procedure for computing crystal shapes from XRD data is sketched in Table 1, illustrating it with cerium oxide[40] as a specific example. The agreement between the computed crystal shape and the actual shape of CeO_2 found in TEM is excellent.

It should be pointed out that the crystal shape algorithm is applicable to powder as well as single-crystal specimens. In the case of single crystals, the algorithm will capture the exact shape of the single crystal. For powder specimens with particle "shape dispersion", the algorithm will capture the average shape. For the CeO_2 sample in Table 1, it is clear that there is not much shape dispersion and all of the crystals are practically hexagonal. To validate the algorithm against experimentally available crystal shape data, an extensive online search, using Science Direct and ACS websites (www.sciencedirect.com and pubs.acs.org), was undertaken for TEM. More than 1500 journal papers from a spectrum of disciplines were browsed for relevant data. Our criterion for acceptance was that the paper must have good quality XRD data and TEM data for one and the same specimen. Using this criterion, we could select only seven papers from nearly 1500 papers for validating our shape algorithm. Apart from the CeO_2 example presented in Table 1, we have carried out six more validations on the following systems: Ge,[41] ZnO,[42] $Zr_{56}C_{44}$,[43] In_2O_3,[44] $MnFe_2O_4$,[2] and iron(II−III) hydroxysulfate.[45] Four of them are presented in Figure 1, while the remaining two are collected in the Supporting Information. Figure 1a,b shows data pertaining to nanocrystals of germanium. These cubic nanocrystals were synthesized using the surfactant

Table 1. Detailed Sketch of the Procedure for Computing Crystal Shape from XRD Data with CeO_2 as an Example[a]

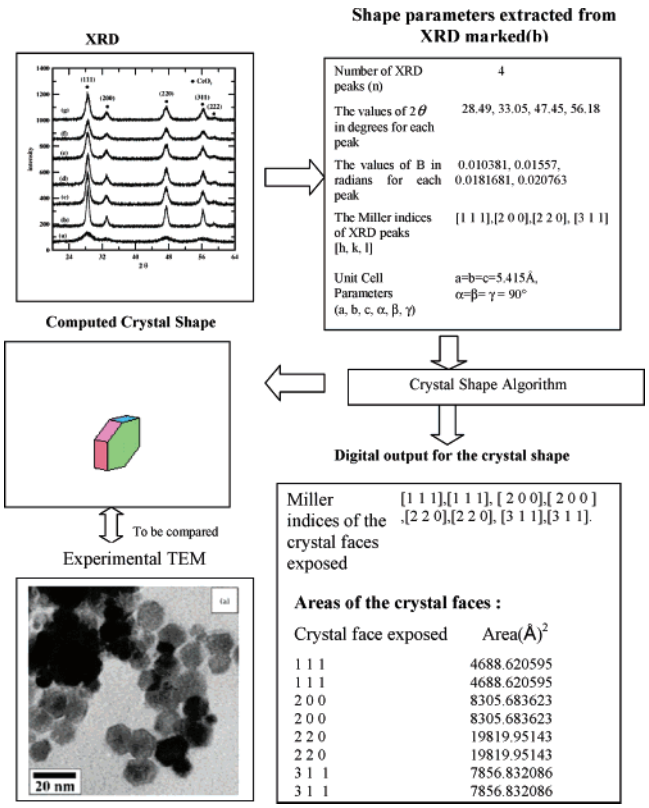

[a] The XRD and TEM are reproduced with permission from ref 40. Copyright 2004 Elsevier.

$C_{12}E_7$ as a shape-controlling agent.[41] Figure 1c is the computed crystal shape of ZnO validated against the available TEM data[42] shown in Figure 1d. Though one or two crystals are distorted from the perfect hexagonal shape, the overall agreement with the computed crystal shape is evident. Note further that the two crystals that cut the picture frame at the lower right corner do possess the hexagonal shape. Figure 1e,f has the data on In_2O_3.[44] It is evident from the TEM photograph that most particles have square or rhombohedral shape, agreeing with shape generated by our algorithm. Figure 1g,h shows, respectively, the computed crystal shape and TEM of $MnFe_2O_4$.[2] The TEM shows the top view for all the "cubelike" crystals. Note further that the crystals have identical shapes and nearly the same sizes. Unlike the TEM showing the crystals lying flat, the computed crystal shape has the "depth" information in it, with the top face having more area than the side faces. During our extensive online search for shape data for validating our algorithm, STM and AFM data were also encountered, besides TEM data. However, STM and AFM provided a hazy view of conglomerated crystals pinned to a substrate, and the individual crystal shapes could not be elucidated. Therefore, we have used only TEM data for validation.

Discussion and Conclusion

We have developed for the first time an elegant mathematical method for computing 3D crystal shapes of materials from X-ray diffraction data. The invented algorithm was applied to cubic, tetragonal, and hexagonal crystal systems, though not restricted to these. The method was illustrated by generating several interesting crystal shapes that were further validated by compar-

ing the computed shapes with the shapes found using TEM. We believe that this method will be extremely useful for characterizing the crystal shapes of material powders and for elucidating shape−property correlations. It will also help to confirm the predictions of crystal shape models because one can synthesize any given material under varying experimental conditions (of temperature, pH, solvent and surfactants, etc), take the XRD, and analyze the crystal shape using the proposed method. It must be emphasized here that while the theoretical approaches reviewed above aim to predict crystal shapes, the present method aims to find crystal shapes actually present in real material specimens. In principle, the said method is applicable to powder XRD as well as single-crystal XRD and to nanosized as well as microsized particles. Nonetheless, two probable limitations should be kept in mind. First, if the particle size is too small, the Scherrer formula might be stretched to its limit of validity,[52] and second, if the particle size is too large, applications of corrections to XRD peak broadening arising from instrumental and other extraneous sources might become tricky. Hence adequate caution must be exercised to ensure that the full widths at half-maximum extracted from XRD data are free from such artifacts.

The present method is equally applicable to organics though the validation examples provided in this paper are limited to inorganics. It must be mentioned, however, that indexing X-ray powder data for organic solids with a small particle size (and other nanomaterials) may pose a problem. The wide and overlapping XRD peaks, which may be present, should be carefully resolved and indexed before applying the crystal shape algorithm to them.[53] In the second phase of our work, we propose to study organic/biological systems and take a closer look at some of these issues.

The present algorithm is also, interestingly, complementary to TEM in that, in the presence of agglomeration of individual crystallites, TEM captures the shapes of only the agglomerates, while our algorithm captures the shapes of the crystallites constituting the agglomerate. For the same reason, caution must be exercised in comparing the shape found using the present algorithm with that found by TEM. Once the exposed crystal faces (i.e., their Miller indices) are found by our algorithm, the atomic arrangement on the crystal faces can be readily found using any of the available softwares, for example, CASTEP of the Materials Studio group of softwares. The atomic arrangement on the crystal face is, in turn, the starting point for elucidating a host of surface properties and processes (e.g., binding site, binding energy, and surface reaction rates). Figure 5 in Supporting Information shows the atomic arrangements of cerium and oxygen in the four exposed crystal faces ([1 1 1], [2 0 0], [2 2 0], [3 1 1]) of CeO_2 crystal found using the present algorithm.

It must be further pointed out that in the present work the simple Scherrer formula with a constant Scherrer constant was used. Langford[47] et al. reported that the Scherrer constant may depend on the {*hkl*} and Varges[48] et al. reported that the Scherrer constant depends on the crystal shape also. Hence, refinements of the present algorithm are clearly possible. When quantitative relations between the Miller index, the shape, and the Scherrer constant become available, a shape refinement process will be possible using the following iteration: start with {*hkl*}-dependent Scherrer constants → find the first approximation to the crystal shape (using the present algorithm) → include the shape information in the Scherrer constants → iterate. This refinement process for the crystal shape will be similar to the Rietveld refinement for the internal crystal structure determination. For future work on the crystal shape problem, we are also presently looking at the possibility (though looking formidable) of a Fourier analysis based method that may eventually do away with the Scherrer formula. It is appropriate here to mention the work of Hall[49] et al. who compute the diffraction profile using the Debye function analysis for selected models of nanocrystal shapes. While this is a direct problem, ours is the corresponding indirect problem for computing crystal shapes from X-ray diffraction data. There is scope for fruitfully combining Hall's approach with our present approach to refine the crystal shape elucidation. The fact that the simple Scherrer-formula-based algorithm has produced fairly good agreement with TEM data shows that, though the shape refinement will certainly be desirable, the present algorithm is not far from reality. It may also be worthwhile to explore the applicability of the present method to neutron and electron diffraction data given the similarities of the underlying physical principles with the X-ray diffraction.

Supporting Information Available: Details of the mathematical algorithm and figures depicting the determined crystal shapes and corresponding TEM images for iron(II−III) hydroxysulfate and $Zr_{56}C_{44}$, crystal shapes determined for Mo_2C, FePt, and VN, crystal habits of NaCl crystals in varying concentrations of urea, and the atomic arrangements of cerium and oxygen in the four exposed crystal faces ([1 1 1], [2 0 0], [2 2 0], [3 1 1]) of CeO_2 crystal found using the present algorithm. This material is available free of charge via the Internet at http://pubs.acs.org.

References

(1) Ma, Y.; Qi, L.; Ma, J.; Cheng, H. *Cryst. Growth Des.* **2004**, *4*, 351.
(2) Zeng, H.; Rice, P. M.; Wang, S. X.; Sun, S. *J. Am. Chem. Soc.* **2004**, *126*, 11458.
(3) Hu, J.; Li, L.; Yang, W.; Manna, L.; Wang, L.; Alivisatos, A. P. *Science* **2001**, *292*, 2060.
(4) Xiong, Y.; Chen, J.; Wiley: B.; Xia, Y.; Aloni, S.; Yin, Y. *J. Am. Chem. Soc.* 2**005**, *127*, 7332.
(5) Yin, Y.; Rioux, R. M.; Erdonmez, C. K.; Hughes, S.; Somorjai, G. A.; Alivisatos, A. P. *Science* **2004**, *304*, 711. [Please see also references cited in ref 4].
(6) Bradley, J. S.; Tesche, B.; Busser, W.; Maase, M.; Reetz, M. T. *J. Am. Chem. Soc.* **2000**, *122*, 4631.
(7) Gugliotti, L. A.; Feldheim, D. L.; Eaton, B. E. *Science* **2004**, *304*, 850.
(8) Narayanan, R.; El-Sayed, M. A. *J. Phys. Chem. B* **2005**, *109*, 12663 and references therein.
(9) Peng, X.; Manna, L.; Yang, W.; Wickham, J.; Scher, E.; Kadavanich, A.; Alivisatos, A. P. *Nature* **2000**, *404*, 59.
(10) Weerd, J.v.d.; Kazarian, S. G. *J. Controlled Release* **2004**, *98*, 295.
(11) Fujiwara, M.; Nagy, Z. K.; Chew, J. W.; Braatz, R. D. *J. Process Control* **2005**, *15*, 493.
(12) Checa, A. G.; Rodríguez-Navarro, A. B. *Biomaterials* **2005**, *26*, 1071.
(13) Walton, R. C.; Kavanagh, J. P.; Heywood, B. R.; Rao, P. N. *Biochim. Biophys. Acta* **2005**, *1723*, 175.
(14) Checa, A. G.; Rodríguez-Navarro, A. B.; Esteban-Delgado, F. J. *Biomaterials* **2005**, *26*, 6404.
(15) Ristic, R. I.; Finnie, S.; Sheen, D. B.; Sherwood, J. N. *J. Phys. Chem. B* **2001**, *105*, 9057.
(16) Sra, K. A.; Ewers, T. D.; Schaak, R. E. *Chem. Mater.* **2005**, *17*, 758.
(17) Luo, F.; Jia, C.-J.; Song, W.; You, L.-P.; Yan, C.-H. *Cryst. Growth Des.* **2005**, *5*, 137.
(18) Hirnao, M.; Morikawa, H. *Chem. Mater.* **2003**, *15*, 2561.
(19) Fang, Y.-P.; Xu, A.-W.; Qin, A.-M.; Yu, R.-J. *Cryst. Growth Des.* **2005**, *5*, 1221.
(20) Jun, Y.-W.; Casula, M. F.; Sim, J.-H.; Kim, S. Y.; Cheon, J.; Alivisatos, A. P. *J. Am. Chem. Soc.* **2003**, *125*, 15981.
(21) Paglia, G.; Buckley, C. E.; Rohl, A. L.; Hart, R. D.; Winter, K.; Studer, A. J.; Hunter, B. A.; Hanna, J. V. *Chem. Mater.* **2004**, *16*, 220.
(22) Suyal, G.; Colla, E.; Gysel, R.; Cantoni, M.; Setter, N. *Nano Lett.* **2004**, *4*, 1339.
(23) Braybrook, A. L.; Heywood, B. R.; Jackson, R. A.; Pitt, K. *J. Cryst. Growth* **2002**, *243*, 336.

(24) Filankembo, A.; Giorgio, S.; Lisiecki, I.; Pileni, M. P. *J. Phys. Chem. B* **2003**, *107*, 7492.
(25) Lu, Z.; Tang, Y.; Chen, L.; Li, Y. *J. Cryst. Growth* **2004**, *266*, 539.
(26) Fogg, A. M.; Freij, A. J.; Rohl, A. L.; Ogden, M. I.; Parkinson, G. M. *J. Phys. Chem B* **2002**, *106*, 5820.
(27) Song, H.; Kim, F.; Connor, S.; Somorjai, G. A.; Yang, P. *J. Phys. Chem. B* **2005**, *109*, 188.
(28) Orme, C. A.; Noy, A.; Wierzbicki, A.; McBride, M. T.; Grantham, M.; Teng, H. H.; Dove, P. M.; DeYoreo, J. J. *Nature* **2001**, *411*, 775.
(29) Phillips, F. C. *An Introduction to crystallography*; The University Press: Glasgow, Scotland, 1971.
(30) Oura, K.; Lifshits, V. G.; Saranin, A. A.; Zotov, A. V.; Katayama, M. *Surface Science An Introduction*; Spinger-Verlag: NewYork, 2003.
(31) Kitayama, M.; Glaeser, A. M. *J. Am. Ceram. Soc.* **2002**, *85*, 611.
(32) Ramanujan, R. V. *Mater. Sci. Eng. B* **1995**, *32*, 125.
(33) Docherty, R.; Clydesdale, G.; Roberts, K. J.; Bennema, P. *J. Phys. D: Appl. Phys.* **1991**, *24*, 89.
(34) Lu, J. J.; Ulrich, J. *Cryst. Res. Technol.* **2003**, *38*, 63.
(35) Myerson, A. S. In *Molecular modeling applications in crystallization*; Docherty, R., Meenan, P., Eds.; Cambridge University Press: New York, 1999.
(36) Hartman, P.; Bennema, P. *J. Cryst. Growth* **1980**, *49*, 145.
(37) Liu, X. Y.; Boek, E. S.; Briels, W. J.; Bennema, P. *Nature* **1995**, *374*, 342.
(38) Bisker-Leib, V.; Doherty, M. F. *Cryst. Growth Des.* **2003**, *3*, 221.
(39) Sweegers, C.; Boerrigter, S. X. M.; Grimbergen, R. F. P.; Meekes, H.; Fleming, S.; Hiralal, I. D. K.; Rijkeboer, A. *J. Phys. Chem. B* **2002**, *106*, 1004.
(40) Chen, H.-I.; Chang, H.-Y. *Colloids Surf., A* **2004**, *242*, 61.
(41) Wang, W. Z.; Huang, J. Y.; Ren, Z. F. *Langmuir* **2005**, *21*, 751.
(42) Hwang, C.-C.; Wu, T.-Y. *Mater. Sci. Eng., B* **2004**, *111*, 197.
(43) Mahday, A. A.; El-Eskandarany, M. S.; Ahmed, H. A.; Amer, A. A. *J. Alloys Compd.* **2000**, *299*, 244.
(44) Zhao, Y.; Zhang, Z.; Wu, Z.; Dang, H. *Langmuir* **2004**, *20*, 27.
(45) Géhin, A.; Ruby, C.; Abdelmoula, M.; Benali, O.; Ghanbaja, J.; Refait, P.; Génin, J. R. *Solid State Sci*. **2002**, *4*, 61.
(46) Borchert, H.; Shevchenko, E. V.; Robert, A.; Mekis, I.; Kornowski, A.; Grubel, G.; Weller, H. *Langmuir* **2005**, *21*, 1931.
(47) Langford, J. I.; Wilson, A. J. C. *J. Appl. Crystallogr.* **1978**, *11*, 102.
(48) Vargas, R.; Louer, D.; Langford, J. I. *J. Appl. Crystallogr.* **1983**, *16*, 512.
(49) Hall, B. D. *J. Appl. Phys.* **2000**, *87*, 1666 and references therein.
(50) The internal crystal structure should clearly be distinguished from the external shape considered in this paper.
(51) In addition, the crystal system information is also required for computing the interplanar separation d_{hkl} entering the algorithm.
(52) The applicability of the simple Scherrer formula has been checked[46] for nanocrystals of size down to 10 nm.
(53) We thank an anonymous reviewer for useful comments in this regard.

CG060052L